

Theory-Data Comparisons for Jet Measurements in Hadron-Induced Processes

The fastNLO Collaboration

M. Wobisch

Louisiana Tech University, Ruston, Louisiana, USA

D. Britzger

DESY, Hamburg, Germany

T. Kluge

University of Liverpool, U.K.

K. Rabbertz, F. Stober

KIT, Karlsruhe, Germany

September 6, 2011

Abstract

We present a comprehensive overview of theory-data comparisons for inclusive jet production. Theory predictions are derived for recent parton distribution functions and compared with jet data from different hadron-induced processes at various center-of-mass energies \sqrt{s} . The comparisons are presented as a function of jet transverse momentum p_T or, alternatively, of the scaling variable $x_T = 2p_T/\sqrt{s}$.

1 Introduction

In this article we provide a comprehensive overview of theory-data comparisons for inclusive jet cross section measurements made in hadron-induced processes between 1993 and today. The comparisons are made for the central region in (pseudo-) rapidity. Data sets include inclusive jet cross sections measured in hadron-hadron collisions at center-of-mass energies \sqrt{s} between 200 GeV and 7 TeV and in deeply inelastic scattering (DIS) at $\sqrt{s} = 300$ GeV and 318 GeV. The theory calculations are computed consistently for all data sets using recent parton distribution functions (PDFs) and common choices for the strong coupling constant $\alpha_s(M_Z)$ and the renormalization and factorization scales. Ratios of data and theory are presented as a function of jet transverse momentum¹ p_T or, alternatively, as a function of the scaling variable $x_T = 2p_T/\sqrt{s}$.

¹Some of the measurements discussed in this article have been made as a function of jet transverse energy E_T . Throughout this article we use p_T to refer to both, either the jet transverse momentum or the jet transverse energy, as appropriate. In hadron-hadron collisions, “transverse” refers to the momentum or energy component perpendicular to the hadron-hadron beam axis. In DIS, “transverse” refers to the momentum component perpendicular to the photon-proton axis (which is the z -axis in the Breit frame).

This article is intended as a persistent repository for the newest theory-data comparisons possible in jet production in hadron-induced processes and will be updated whenever new relevant data and/or theory results are published.

In section 2 we discuss how the theory results are obtained while details of the data sets are described in section 3. Comparisons of theory and data are presented in section 4.

2 Theory Predictions

Conventionally, experimental measurements are corrected for instrumental effects and the results are provided at the “particle level” [1]. Corresponding theory predictions for jet observables O_{theory} are therefore obtained as the product of a perturbative QCD (pQCD) result, O_{pQCD} , multiplied by a correction factor for non-perturbative effects, $c_{\text{non-pert}}$

$$O_{\text{theory}} = O_{\text{pQCD}} \cdot c_{\text{non-pert}} . \quad (1)$$

For inclusive jet cross sections in hadron-hadron collision and in DIS, the fixed-order perturbative expansion is known to next-to-leading order (NLO) in the strong coupling constant α_s , which is of order $\mathcal{O}(\alpha_s^2)$ for DIS and $\mathcal{O}(\alpha_s^3)$ for hadron-hadron collisions. For inclusive jet cross sections in hadron-hadron collisions, additional $\mathcal{O}(\alpha_s^4)$ corrections from threshold corrections have been computed [2]. These results are used for the calculations in this article. Renormalization and factorization scales, μ_r and μ_f , are set to $\mu_r = \mu_f = p_T$, where p_T is the transverse momentum (or, where appropriate, transverse energy) of the individual jet. In all cases μ_r and μ_f are larger than the b-quark mass, and thus all calculations are made for five active flavors ($n_f = 5$). The proton PDFs are taken from the PDF parametrizations MSTW2008 [3], CT10 [4], NNPDF2.1 [5], or HERAPDF1.5 [6, 7]. All of these parametrizations are available in NLO and NNLO approximations (except for CT10 which are only available in NLO) as well as for a series of $\alpha_s(M_Z)$ values. In each case, we use those PDF sets which were obtained for $\alpha_s(M_Z) = 0.118$ which is closest to the current world average value [8]. The same value of $\alpha_s(M_Z)$ is also employed in the matrix elements. The NLO PDF parametrizations are used for the comparisons with DIS data, together with the NLO matrix elements. The NNLO versions (where available) are used for the comparisons with data from hadron-hadron collisions, together with NLO matrix elements plus $\mathcal{O}(\alpha_s^4)$ contributions from threshold corrections. Correspondingly, in these comparisons α_s is evolved using the numerical solutions of the 2-loop and 3-loop approximations of the renormalization group equation for DIS and hadron-hadron collisions, respectively. All pQCD contributions are computed within the framework of fastNLO [9] using NLOJET++ [10, 11] for the LO and NLO contributions and code from the authors of Ref. [2] for the threshold corrections. The anti- k_T jet algorithm is taken from the implementation in FASTJET [12].

The factor $c_{\text{non-pert}}$ includes non-perturbative corrections due to hadronization and the underlying event. These corrections are usually obtained using Monte Carlo event generators and the values are published together with the measurement results. Whenever this was not the case, we have computed the correction factors ourselves using PYTHIA 6.4 [13] with tune A [14]. For DIS data at high Q^2 , underlying event corrections are assumed to be negligible. In those cases, the pQCD results are only corrected for hadronization effects.

For some of the data sets, additional theoretical effects have already been folded into the published results. This is taken into account as follows:

- For some $p\bar{p}$ data sets (as mentioned in section 3), corrections for the underlying event have already been applied to the data. In the corresponding calculations, pQCD theory is only corrected for hadronization effects.
- Observables in DIS are usually corrected for higher order QED effects which may either include corrections for the running of the QED coupling α , or not. The former is the standard choice by the ZEUS Collaboration, and therefore the corresponding pQCD calculations are made for a fixed value of $\alpha = 1/137$. Jet measurement results from the H1 Collaboration are not corrected for the running of α , and therefore the corresponding pQCD calculations include a running value of $\alpha(Q)$.

3 Data Sets

In this section, we give a brief overview on the data sets which are used in the theory-data comparisons. The phase space requirements are given as stated in the cited publications which include further details regarding the exact definition of the variables. The recombination schemes used in the jet algorithms are usually the E -scheme [15], or the E_T -scheme (frequently referred to as “Snowmass convention”) [16]. In some cases other recombination schemes have been used. The following measurements of the inclusive jet cross section as a function of p_T are used in the comparisons. All data are corrected to the particle level as defined in Ref. [1], except where mentioned otherwise.

1. Proton-proton scattering at $\sqrt{s} = 7$ TeV at the LHC
 - (a) CMS Collaboration (2011) $\mathcal{L}_{\text{int}} = 34 \text{ pb}^{-1}$ [17]
Measurement of $d^2\sigma/dp_T dy$ for $18 < p_T < 1100$ GeV in six rapidity regions $|y| < 3.0$ using the anti- k_T jet algorithm with $R = 0.5$ in the E -scheme. In our comparisons we display the results for $|y| < 0.5$. Non-perturbative corrections are determined as the average of PYTHIA 6.422 with tune D6T [18] and HERWIG++ 2.4.2 [19] with the default tune of HERWIG++ 2.3 (as detailed in Ref. [20]).
 - (b) ATLAS Collaboration (2010) $\mathcal{L}_{\text{int}} = 17 \text{ nb}^{-1}$ [21]
Measurement of $d^2\sigma/dp_T dy$ for $60 < p_T < 500$ GeV in five rapidity regions $|y| < 2.8$ using the anti- k_T jet algorithm with $R = 0.4$ in the E -scheme. In our comparisons we display the results for $0 < |y| < 0.3$. Non-perturbative corrections are determined using PYTHIA 6 with tune MC09.
 - (c) ATLAS Collaboration (2010) $\mathcal{L}_{\text{int}} = 17 \text{ nb}^{-1}$ [21]
The same as in 1. (b), but for $R = 0.6$.
2. Proton-anti-proton scattering at $\sqrt{s} = 1.96$ TeV at the Fermilab Tevatron collider
 - (a) CDF Collaboration (2008) $\mathcal{L}_{\text{int}} = 1.13 \text{ fb}^{-1}$ [22]
Measurement of $d^2\sigma/dp_T dy$ for $62 < p_T < 700$ GeV in five rapidity regions $|y| < 2.1$ using the Run II iterative midpoint cone jet algorithm (CDF version) with $R = 0.7$ in the E -scheme. In our comparisons we display the results for $0.1 < |y| < 0.7$. Non-perturbative corrections are determined using PYTHIA with tune A.
 - (b) CDF Collaboration (2007) $\mathcal{L}_{\text{int}} = 1.0 \text{ fb}^{-1}$ [23]
Measurement of $d^2\sigma/dp_T dy$ for $52 < p_T < 700$ GeV in five rapidity regions $|y| <$

2.1 using the inclusive k_T jet algorithm with $R = 0.7$ in the E -scheme. In our comparisons we display the results for $0.1 < |y| < 0.7$. Non-perturbative corrections are determined using PYTHIA with tune A.

- (c) DØ Collaboration (2008) $\mathcal{L}_{\text{int}} = 0.7 \text{ fb}^{-1}$ [24]
Measurement of $d^2\sigma/dp_T dy$ for $50 < p_T < 600 \text{ GeV}$ in six rapidity regions $|y| < 2.4$ using the Run II iterative midpoint cone jet algorithm (DØ version) with $R = 0.7$ in the E -scheme. In our comparisons we display the results for $|y| < 0.4$. Non-perturbative corrections are determined using PYTHIA with tune QW [25].

3. Proton-anti-proton scattering at $\sqrt{s} = 1.8 \text{ TeV}$ at the Fermilab Tevatron collider

- (a) CDF Collaboration (2001) $\mathcal{L}_{\text{int}} = 10 \text{ pb}^{-1}$ [26]
Measurement of $d^2\sigma/dE_T d\eta$ for $40 < E_T < 465 \text{ GeV}$ in the pseudorapidity range $0.1 < |\eta| < 0.7$ using the JETCLU iterative cone jet algorithm with $R = 0.7$ in a special recombination scheme described in equations (3-9) in [26]. Corrections for the effects due to the underlying event have been estimated using ambient energy measured in minimum bias events and applied to the data. Hadronization corrections have not been published.
- (b) DØ Collaboration (2001) $\mathcal{L}_{\text{int}} = 95 \text{ pb}^{-1}$ [27]
Measurement of $d^2\sigma/dE_T d\eta$ for $60 < E_T < 500 \text{ GeV}$ in five pseudorapidity regions $|\eta| < 3.0$ using the DØ Run I iterative cone jet algorithm with $R = 0.7$ in a special recombination scheme, but with additional corrections of jet η to account for the differences to the E_T -scheme [28]. In our comparisons we display the results for $|\eta| < 0.5$. Corrections for the effects due to the underlying event have been estimated using low luminosity minimum bias data [29] and applied to the data. Hadronization corrections have not been published.

4. Proton-anti-proton scattering at $\sqrt{s} = 546, 630 \text{ GeV}$ at the Fermilab Tevatron collider

- (a) CDF Collaboration (1993) at $\sqrt{s} = 546 \text{ GeV}$, $\mathcal{L}_{\text{int}} = 8.58 \text{ nb}^{-1}$ [30]
Measurement of $d^2\sigma/dE_T d\eta$ for $27.5 < E_T < 73 \text{ GeV}$ in the pseudorapidity range $0.1 < |\eta| < 0.7$ using the JETCLU iterative cone jet algorithm with $R = 0.7$ in a special recombination scheme, described in equations (3-9) in [26]. Corrections for effects due to the underlying event have been estimated using the observed calorimeter transverse energy at 90° to the jet axis in CDF dijet events and applied to the data. Hadronization corrections have not been published.
- (b) DØ Collaboration (2001) $\sqrt{s} = 630 \text{ GeV}$, at $\mathcal{L}_{\text{int}} = 538 \text{ nb}^{-1}$ [31]
Measurement of $d^2\sigma/dE_T d\eta$ for $21 < E_T < 196 \text{ GeV}$ in the pseudorapidity region $|\eta| < 0.5$ using the DØ Run I iterative cone jet algorithm with $R = 0.7$ in a special recombination scheme (see [31]). Corrections for the effects due to the underlying event have been estimated using Monte Carlo simulations of $p\bar{p}$ interactions and applied to the data. Hadronization corrections have not been published.

5. Proton-proton scattering at $\sqrt{s} = 200 \text{ GeV}$ at RHIC

- (a) STAR Collaboration (2006) $\mathcal{L}_{\text{int}} = 0.30 \text{ pb}^{-1}$ [32]
Measurement of $d^2\sigma/dp_T d\eta$ for $5 < p_T < 49 \text{ GeV}$ in the pseudorapidity region $0.2 < |\eta| < 0.8$ using the Run II iterative midpoint cone jet algorithm (implemented following [15]) with $R = 0.7$ in the E -scheme. Non-perturbative

corrections have not been published. Those were provided to us by one of the authors [33].

6. Deeply inelastic scattering at $\sqrt{s} = 318$ GeV at HERA

- (a) H1 Collaboration (2007) $\mathcal{L}_{\text{int}} = 65.4 \text{ pb}^{-1}$ [34]
 Measurement of $d^2\sigma/dE_T dQ^2$ for $7 < E_T < 50$ GeV and $150 < Q^2 < 15000$ GeV² at an inelasticity $0.2 < y < 0.7$ in the pseudorapidity region $-1 < \eta_{\text{lab}} < 2.5$ using the inclusive k_T jet algorithm in the Breit frame with $R = 1$ in the E_T -scheme. In these comparisons we are using the data $150 < Q^2 < 5000$ GeV² for which contributions from Z exchange are negligible. The data have been corrected to the particle level and for QED radiative corrections, but not for the running of α . Hadronization corrections have been determined as the average value using DJANGO [35] and RAPGAP [36].
- (b) ZEUS Collaboration (2007) $\mathcal{L}_{\text{int}} = 81.7 \text{ pb}^{-1}$ [37]
 Measurement of $d^2\sigma/dE_T dQ^2$ for $8 < E_T < 100$ GeV and $Q^2 > 125$ GeV² with $|\cos \gamma_h| < 0.65$ in the pseudorapidity region $-2 < \eta_{\text{Breit}} < 1.5$ using the inclusive k_T jet algorithm in the Breit frame with $R = 1$ in the E_T -scheme. In these comparisons we are using the data $125 < Q^2 < 5000$ GeV² for which contributions from Z exchange are negligible. The data have been corrected to particle level and for QED radiative corrections, including the running of α . Hadronization corrections have been determined as the average value using ARIADNE [38, 39] and LEPTO [40].

7. Deeply inelastic scattering at $\sqrt{s} = 300$ GeV at HERA

- (a) H1 Collaboration (2001) $\mathcal{L}_{\text{int}} = 33 \text{ pb}^{-1}$ [41]
 Measurement of $d^2\sigma/dE_T dQ^2$ for $7 < E_T < 50$ GeV and $150 < Q^2 < 5000$ GeV² at $0.2 < y < 0.6$ in the pseudorapidity region $-1 < \eta_{\text{lab}} < 2.5$ using the inclusive k_T jet algorithm in the Breit frame with $R = 1$ in the E_T -scheme. The data have been corrected to particle level and for QED radiative corrections, but not for the running of α . Hadronization corrections have been determined as the average value from HERWIG [42], LEPTO, and ARIADNE.
- (b) ZEUS Collaboration (2002) $\mathcal{L}_{\text{int}} = 10 \text{ pb}^{-1}$ [43]
 Measurement of $d^2\sigma/dE_T dQ^2$ for $8 < E_T < 100$ GeV and $Q^2 > 125$ GeV² with $-0.7 < \cos \gamma_h < 0.5$ in the pseudorapidity region $-2 < \eta_{\text{Breit}} < 1.8$ using the inclusive k_T jet algorithm in the Breit frame with $R = 1$ using the E_T -scheme. In these comparisons we are using the data $125 < Q^2 < 5000$ GeV² for which contributions from Z exchange are negligible. The data have been corrected to particle level and for QED radiative corrections, including the running of α . Hadronization corrections have been determined as the average value using ARIADNE, LEPTO, and HERWIG.

4 Results

The ratios of data and theory for all results obtained in hadron-hadron collisions and in DIS at large four-momentum transfer squared Q^2 , are shown in Fig. 1 as a function of jet p_T . For DIS, the variable p_T corresponds to the jet transverse energy defined in the Breit frame of reference. The uncertainty bars indicate the total experimental uncertainties, defined as the quadratic sum of statistical and systematic uncertainties. For purposes of visibility, the ratios for different center-of-mass energies are multiplied by factors as given in the figures, and the results are sorted from top to bottom in the order of increasing center-of-mass energy.

Figure 2 shows the data points from hadron-hadron collisions, this time as a function of $x_T = 2p_T/\sqrt{s}$. For central jet production in hadron-hadron collisions, the variable x_T is closely related to the hadron momentum fractions x_1 and x_2 , carried by the partons. In exclusive dijet production with rapidities $y_1 = y_2 = 0$, the relation $x_T = x_1 = x_2$ holds.

The comparison of inclusive jet cross section data at central (pseudo-) rapidities as a function of x_T allows to infer the sensitivity of PDF determinations to the measured data.

In general, we observe good agreement between theory and data. The data from some measurements (CDF at $\sqrt{s} = 546$ GeV [30] and ATLAS and CMS at $\sqrt{s} = 7$ TeV [21, 17]) have a tendency of being systematically below the theory predictions. However, the CDF and ATLAS data have relatively large uncertainties, and it was discussed in Refs. [17, 20] that within experimental and theoretical uncertainties, the CMS data are in agreement with theory. Differences in the shapes between theory and data as a function of p_T for the jet data at $\sqrt{s} = 1.8$ and 1.96 TeV can be explained by correlated experimental uncertainties, as studied in recent global PDF analyses [3, 4, 5].

The theory-data comparisons which are presented in Figs. 1 and 2 for MSTW2008 PDFs are also repeated for the PDF parametrizations CT10, NNPDF2.1, and HERAPDF1.5. These results are displayed in Figs. 3 – 8. In most cases we observe a very similar agreement as for MSTW2008 PDFs.

From Fig. 1 it is visible that the new LHC jet data have started to go beyond the p_T reach of the Fermilab Tevatron experiments CDF and DØ. Fig. 2 shows that the new CMS measurement provides the first jet results which probe the PDFs down to $x = 5 \cdot 10^{-3}$. In this x -region, the PDFs are already constrained by data from inclusive DIS experiments. Therefore the comparison of LHC jet data with theory predictions in this overlap region will help to understand uncertainties not related to PDFs. It is also visible from Fig. 2 that currently the Tevatron jet data still have the highest reach in x .

References

- [1] C. Buttar *et al.*, “Accords related to the hadronic final state,” in G. Belanger *et al.* (Eds.), *Les Houches 2007, Physics at TeV colliders*, arXiv:0803.0678 [hep-ph], section 9.
- [2] N. Kidonakis and J. F. Owens, “Effects of higher-order threshold corrections in high-E(T) jet production,” *Phys. Rev. D* **63**, 054019 (2001). [arXiv:hep-ph/0007268].
- [3] A. D. Martin, W. J. Stirling, R. S. Thorne and G. Watt, “Parton distributions for the LHC,” *Eur. Phys. J. C* **63**, 189 (2009). [arXiv:0901.0002 [hep-ph]].

- [4] H. L. Lai *et al.*, “New parton distributions for collider physics,” *Phys. Rev. D* **82**, 074024 (2010), [arXiv:1007.2241 [hep-ph]].
- [5] R. D. Ball *et al.*, “Impact of Heavy Quark Masses on Parton Distributions and LHC Phenomenology,” *Nucl. Phys. B* **849**, 296 (2011), [arXiv:1101.1300 [hep-ph]].
- [6] H1 and ZEUS Collaborations, “PDF fits including HERA-II high Q^2 data (HERA-PDF1.5),” H1prelim-10-142, ZEUS-prel-10-018 (2010).
- [7] H1 and ZEUS Collaborations, “HERAPDF1.5NNLO” (preliminary), H1prelim-11-042, ZEUS-prel-11-002 (2011).
- [8] S. Bethke, “The 2009 World Average of $\alpha_s(M_Z)$,” *Eur. Phys. J. C* **64**, 689 (2009). [arXiv:0908.1135 [hep-ph]].
- [9] T. Kluge, K. Rabbertz and M. Wobisch, “fastNLO: Fast pQCD calculations for PDF fits,” DESY-06-186, FERMILAB-CONF-06-352-E, arXiv:hep-ph/0609285.
- [10] Z. Nagy, “Next-to-leading order calculation of three-jet observables in hadron hadron collision,” *Phys. Rev. D* **68**, 094002 (2003). [arXiv:hep-ph/0307268].
- [11] Z. Nagy, “Three-jet cross sections in hadron hadron collisions at next-to-leading order,” *Phys. Rev. Lett.* **88**, 122003 (2002). [arXiv:hep-ph/0110315].
- [12] M. Cacciari and G. P. Salam, “Dispelling the N^3 myth for the k_t jet-finder,” *Phys. Lett. B* **641**, 57 (2006) [arXiv:hep-ph/0512210].
- [13] T. Sjostrand, P. Eden, C. Friberg, L. Lonnblad, G. Miu, S. Mrenna, E. Norrbin, “High-energy physics event generation with PYTHIA 6.1,” *Comput. Phys. Commun.* **135**, 238-259 (2001). [hep-ph/0010017].
- [14] R. Field, presented at Fermilab ME/MC Tuning Workshop, Fermilab, October 4, 2002. PYTHIA Tune A implies that the following parameters are set in PYTHIA with CTEQ5L PDFs: PARP(67)=4, MSTP(82)=4, PARP(82)=2, PARP(84)=0.4, PARP(85)=0.9, PARP(86)=0.95, PARP(89)=1800, PARP(90)=0.25.
- [15] G. C. Blazey *et al.*, in *Proceedings of the Workshop: “QCD and Weak Boson Physics in Run II”*, edited by U. Baur, R. K. Ellis, and D. Zeppenfeld, Batavia, Illinois (2000). See Section 3.5.
- [16] J. E. Huth, N. Wainer, K. Meier, N. Hadley, F. Aversa, M. Greco, P. Chiappetta, J. P. Guillet *et al.*, “Toward a standardization of jet definitions,” in *Proc. of Research Directions for the Decade, Snowmass 1990*, ed. E. L. Berger (World Scientific, Singapore, 1992).
- [17] S. Chatrchyan *et al.* [CMS Collaboration], “Measurement of the Inclusive Jet Cross Section in pp Collisions at $\sqrt{s} = 7$ TeV,” accepted by *Phys. Rev. Lett.*, [arXiv:1106.0208 [hep-ex]].
- [18] R. Field, “Physics at the Tevatron,” *Acta Phys. Polon.* B39, 2611 (2008).
- [19] M. Bahr, S. Gieseke, M. A. Gigg, D. Grellscheid, K. Hamilton, O. Latunde-Dada, S. Platzer, P. Richardson *et al.*, “Herwig++ Physics and Manual,” *Eur. Phys. J.* **C58**, 639-707 (2008). [arXiv:0803.0883 [hep-ph]].

- [20] K. Rabbertz, [CMS Collaboration], “Comparison of Inclusive Jet and Dijet Mass Cross Sections at $\sqrt{s} = 7\text{ TeV}$ with Predictions of perturbative QCD,” CMS Note 2011-004 (2011).
- [21] G. Aad *et al.* [Atlas Collaboration], “Measurement of inclusive jet and dijet cross sections in proton-proton collisions at 7 TeV centre-of-mass energy with the ATLAS detector,” Eur. Phys. J. **C71**, 1512 (2011). [arXiv:1009.5908 [hep-ex]].
- [22] T. Aaltonen *et al.* [CDF Collaboration], “Measurement of the Inclusive Jet Cross Section at the Fermilab Tevatron p anti-p Collider Using a Cone-Based Jet Algorithm,” Phys. Rev. **D78**, 052006 (2008). [arXiv:0807.2204 [hep-ex]].
- [23] A. Abulencia *et al.* [CDF - Run II Collaboration], “Measurement of the Inclusive Jet Cross Section using the k_T algorithm in $p\bar{p}$ Collisions at $\sqrt{s} = 1.96\text{ TeV}$ with the CDF II Detector,” Phys. Rev. **D75**, 092006 (2007). [hep-ex/0701051].
- [24] V. M. Abazov *et al.* [D0 Collaboration], “Measurement of the inclusive jet cross-section in $p\bar{p}$ collisions at $s^{91/2} = 1.96\text{-TeV}$,” Phys. Rev. Lett. **101**, 062001 (2008). [arXiv:0802.2400 [hep-ex]].
- [25] T. Q. W. Group *et al.*, “Tevatron-for-LHC report of the QCD working group,” [hep-ph/0610012].
- [26] T. Affolder *et al.* [CDF Collaboration], “Measurement of the inclusive jet cross section in $\bar{p}p$ collisions at $\sqrt{s} = 1.8\text{ TeV}$,” Phys. Rev. **D64**, 032001 (2001). [hep-ph/0102074].
- [27] B. Abbott *et al.* [D0 Collaboration], “Inclusive jet production in $p\bar{p}$ collisions,” Phys. Rev. Lett. **86**, 1707-1712 (2001). [hep-ex/0011036].
- [28] L. Babukhadia, “Rapidity dependence of the single inclusive jet cross section in pp collisions at $\text{sqrt}(s)=1.8\text{ TeV}$ with the D0 detector,” Ph.D. Dissertation, University of Arizona, Tucson, Arizona, USA 1999 (unpublished).
- [29] B. Abbott *et al.* [D0 Collaboration], “Determination of the absolute jet energy scale in the D0 calorimeters,” Nucl. Instrum. Meth. A **424** (1999) 352 [arXiv:hep-ex/9805009].
- [30] F. Abe *et al.* [CDF Collaboration], “Comparison of jet production in $\bar{p}p$ collisions at $\sqrt{s} = 546\text{ GeV}$ and 1800 GeV ,” Phys. Rev. Lett. **70**, 1376-1380 (1993).
- [31] B. Abbott *et al.* [D0 Collaboration], “High- p_T jets in $\bar{p}p$ collisions at $\sqrt{s} = 630\text{ GeV}$ and 1800 GeV ,” Phys. Rev. **D64**, 032003 (2001). [hep-ex/0012046].
- [32] B. I. Abelev *et al.* [STAR Collaboration], “Longitudinal double-spin asymmetry and cross section for inclusive jet production in polarized proton collisions at $s^{**}(1/2) = 200\text{-GeV}$,” Phys. Rev. Lett. **97**, 252001 (2006). [hep-ex/0608030].
- [33] Mike Miller, private communication (2006).
- [34] A. Aktas *et al.* [H1 Collaboration], “Measurement of inclusive jet production in deep-inelastic scattering at high Q^{*2} and determination of the strong coupling,” Phys. Lett. **B653**, 134-144 (2007). [arXiv:0706.3722 [hep-ex]].

- [35] K. Charchula, G. A. Schuler, H. Spiesberger, “Combined QED and QCD radiative effects in deep inelastic lepton - proton scattering: The Monte Carlo generator DJANGO6,” *Comput. Phys. Commun.* **81**, 381-402 (1994).
- [36] H. Jung, “Hard diffractive scattering in high-energy e p collisions and the Monte Carlo generator RAPGAP,” *Comput. Phys. Commun.* **86**, 147-161 (1995).
- [37] S. Chekanov *et al.* [ZEUS Collaboration], “Inclusive-jet and dijet cross-sections in deep inelastic scattering at HERA,” *Nucl. Phys.* **B765**, 1-30 (2007). [hep-ex/0608048].
- [38] L. Lonnblad, “ARIADNE version 4: A Program for simulation of QCD cascades implementing the color dipole model,” *Comput. Phys. Commun.* **71**, 15-31 (1992).
- [39] L. Lonnblad, “Rapidity gaps and other final state properties in the color dipole model for deep inelastic scattering,” *Z. Phys.* **C65**, 285-292 (1995).
- [40] G. Ingelman, A. Edin, J. Rathsman, “LEPTO 6.5: A Monte Carlo generator for deep inelastic lepton - nucleon scattering,” *Comput. Phys. Commun.* **101**, 108-134 (1997). [hep-ph/9605286].
- [41] C. Adloff *et al.* [H1 Collaboration], “Measurement and QCD analysis of jet cross-sections in deep inelastic positron - proton collisions at $s^{*(1/2)}$ of 300-GeV,” *Eur. Phys. J.* **C19**, 289-311 (2001). [hep-ex/0010054].
- [42] G. Marchesini, B. R. Webber, G. Abbiendi, I. G. Knowles, M. H. Seymour, L. Stanco, “HERWIG: A Monte Carlo event generator for simulating hadron emission reactions with interfering gluons. Version 5.1 - April 1991,” *Comput. Phys. Commun.* **67**, 465-508 (1992).
- [43] S. Chekanov *et al.* [ZEUS Collaboration], “Inclusive jet cross-sections in the Breit frame in neutral current deep inelastic scattering at HERA and determination of $\alpha(s)$,” *Phys. Lett.* **B547**, 164-180 (2002). [hep-ex/0208037].

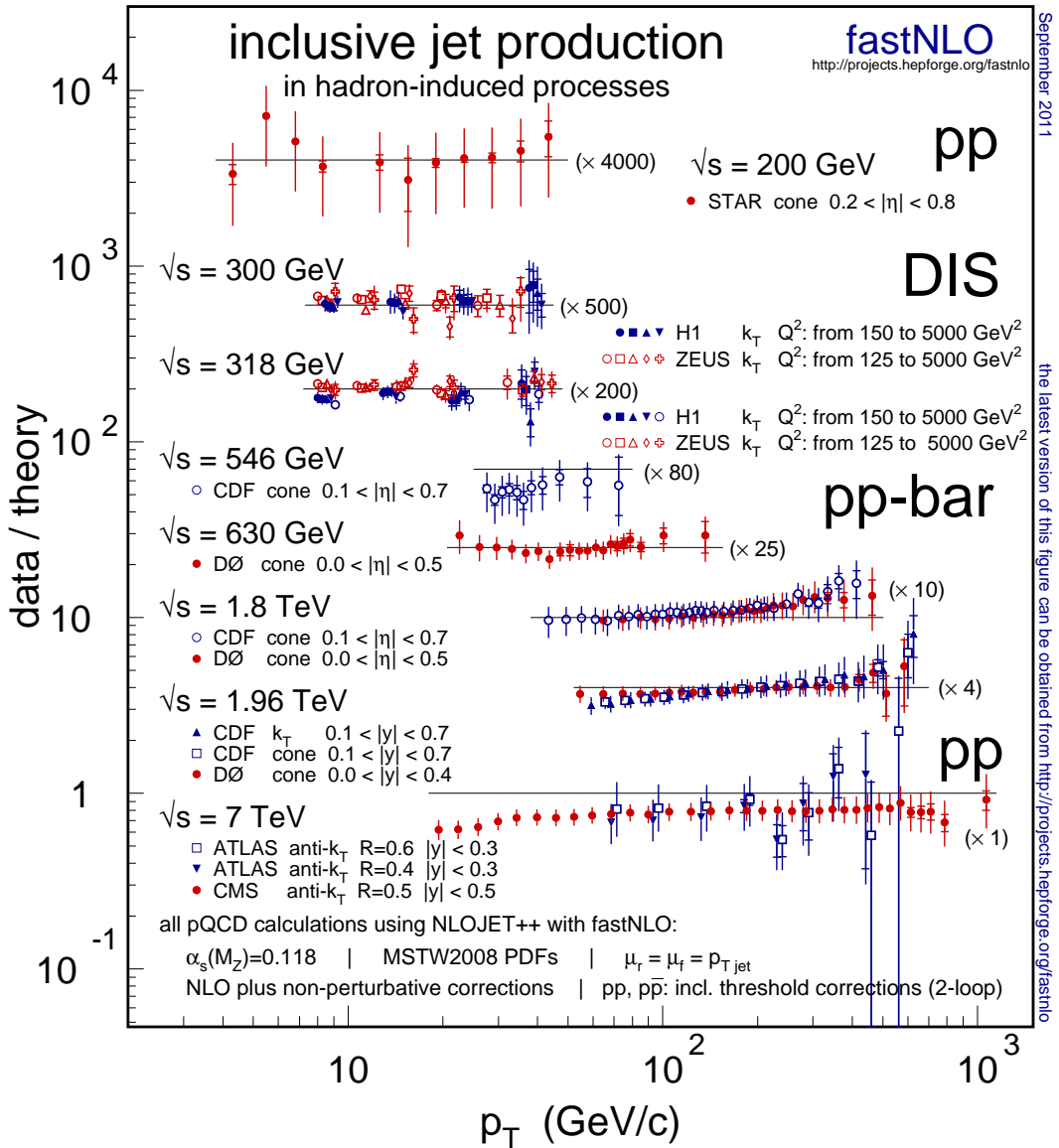


Figure 1: Ratios of data and theory for inclusive jet cross sections measured in hadron-hadron collisions and in deeply inelastic scattering at different center-of-mass energies. The ratios are shown as a function of jet transverse momentum p_T . The theory results are computed for MSTW2008 PDFs.

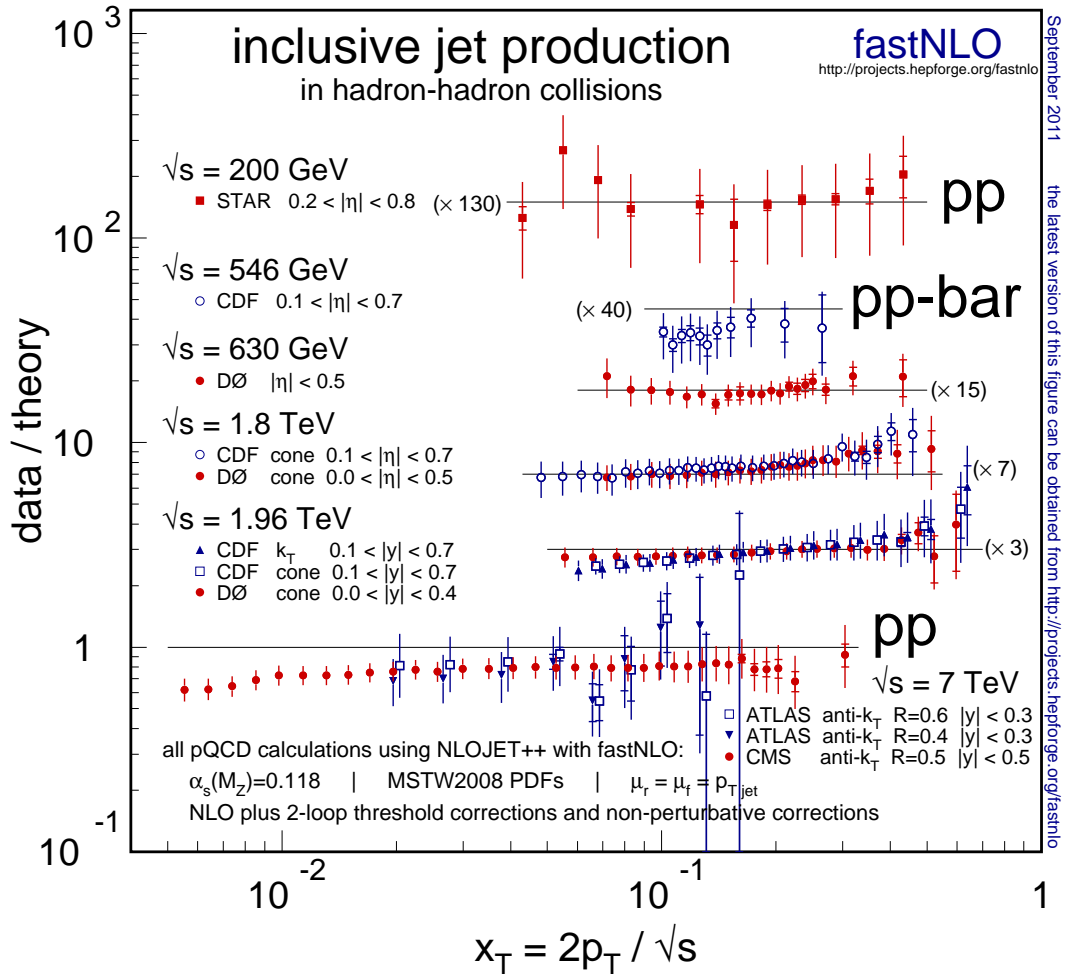


Figure 2: Ratios of data and theory for inclusive jet cross sections measured in hadron-hadron collisions at different center-of-mass energies. The ratios are shown as a function of the scaling variable $x_T = 2p_T / \sqrt{s}$. The theory results are computed for MSTW2008 PDFs.

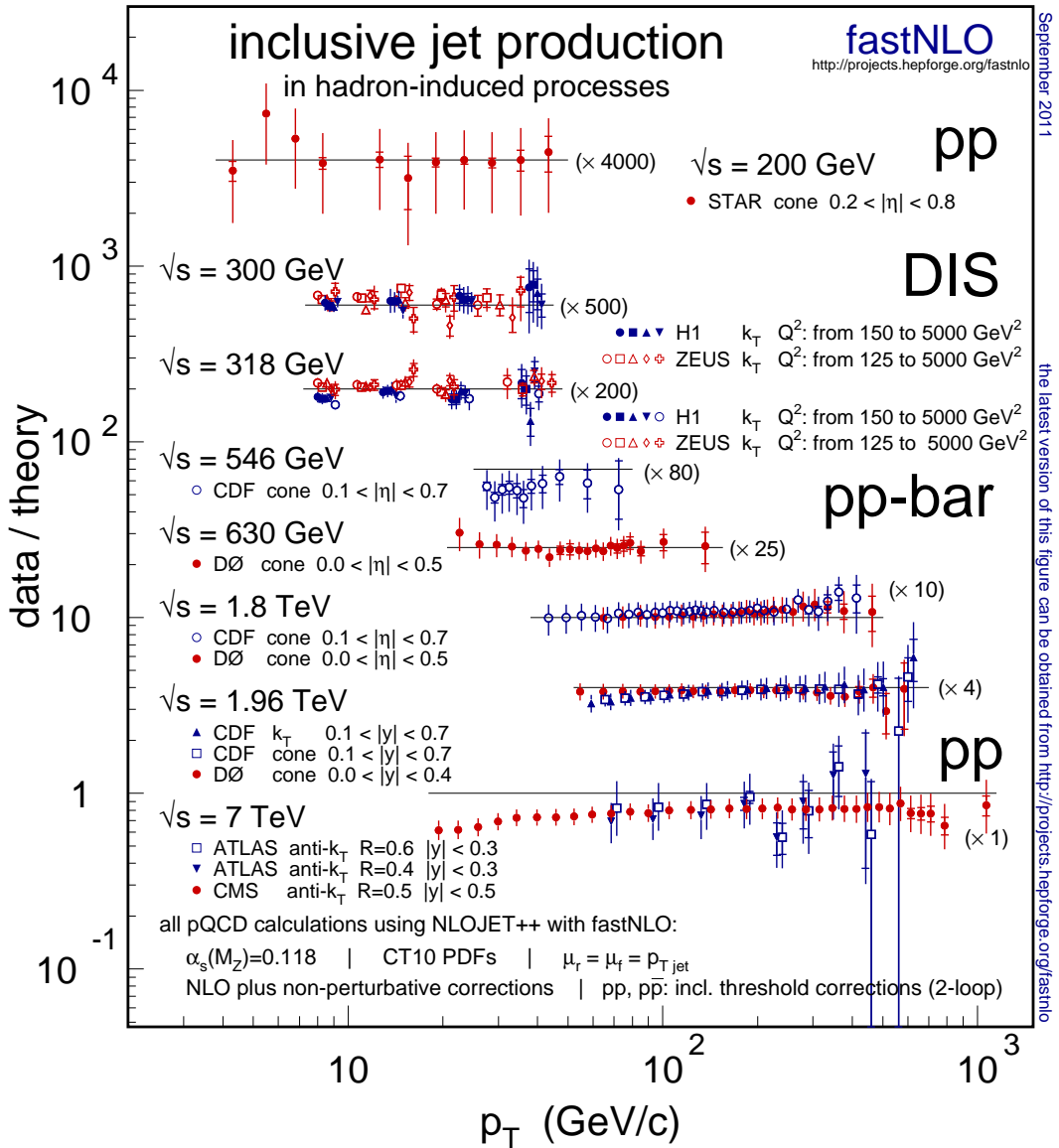


Figure 3: Ratios of data and theory for inclusive jet cross sections measured in hadron-hadron collisions and in deeply inelastic scattering at different center-of-mass energies. The ratios are shown as a function of jet transverse momentum p_T . The theory results are computed for CT10 PDFs.

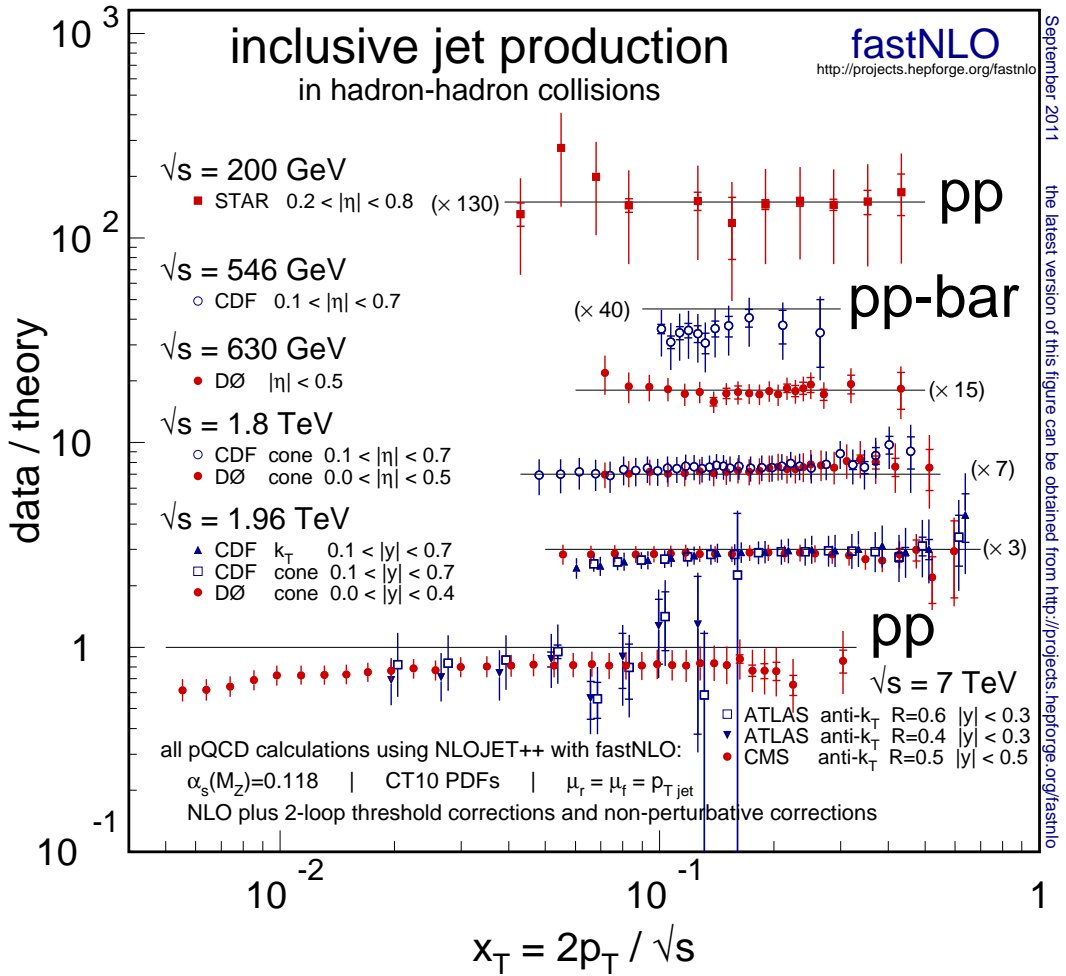


Figure 4: Ratios of data and theory for inclusive jet cross sections measured in hadron-hadron collisions at different center-of-mass energies. The ratios are shown as a function of the scaling variable $x_T = 2p_T / \sqrt{s}$. The theory results are computed for CT10 PDFs.

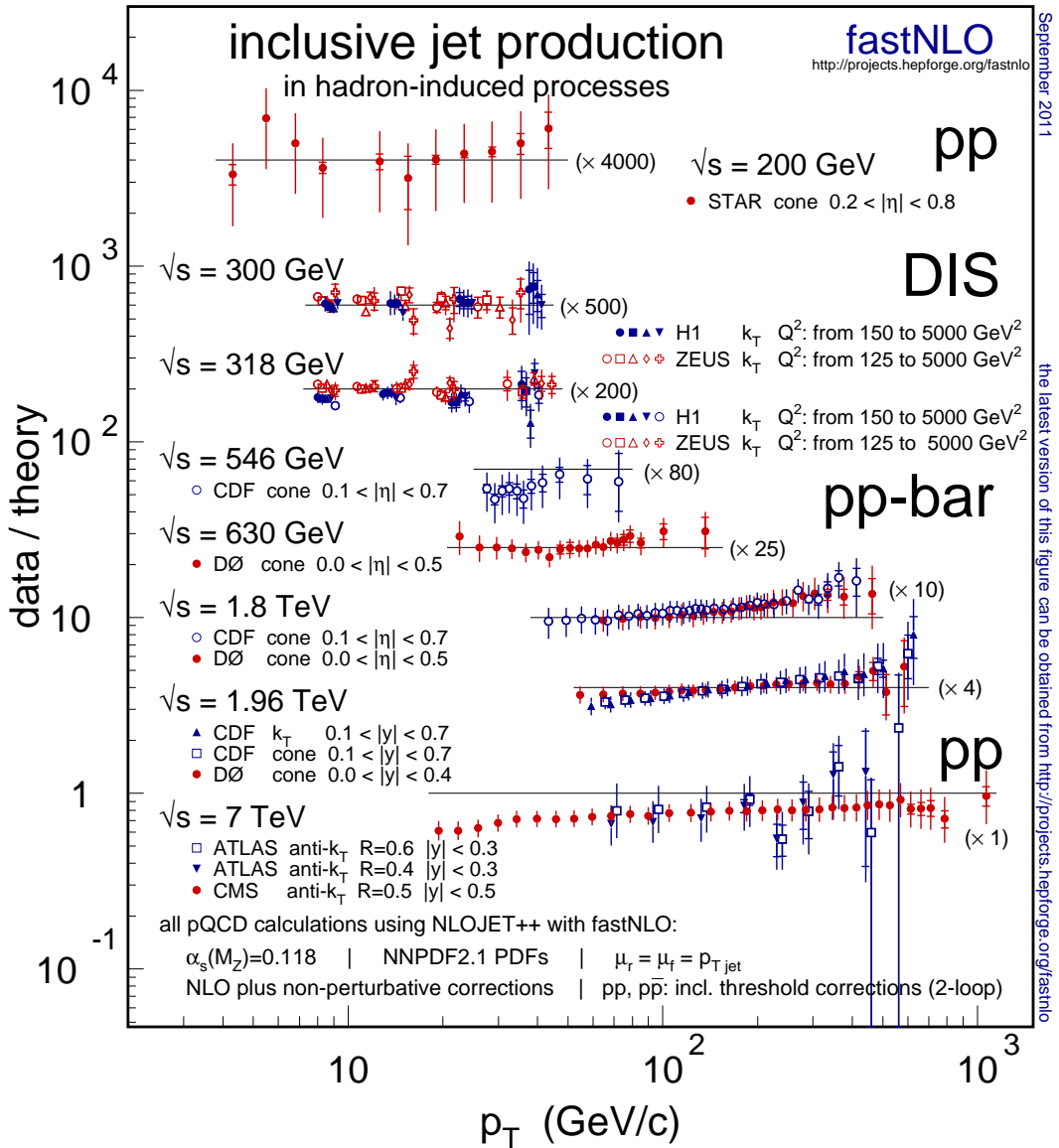


Figure 5: Ratios of data and theory for inclusive jet cross sections measured in hadron-hadron collisions and in deeply inelastic scattering at different center-of-mass energies. The ratios are shown as a function of jet transverse momentum p_T . The theory results are computed for NNPDF2.1 PDFs.

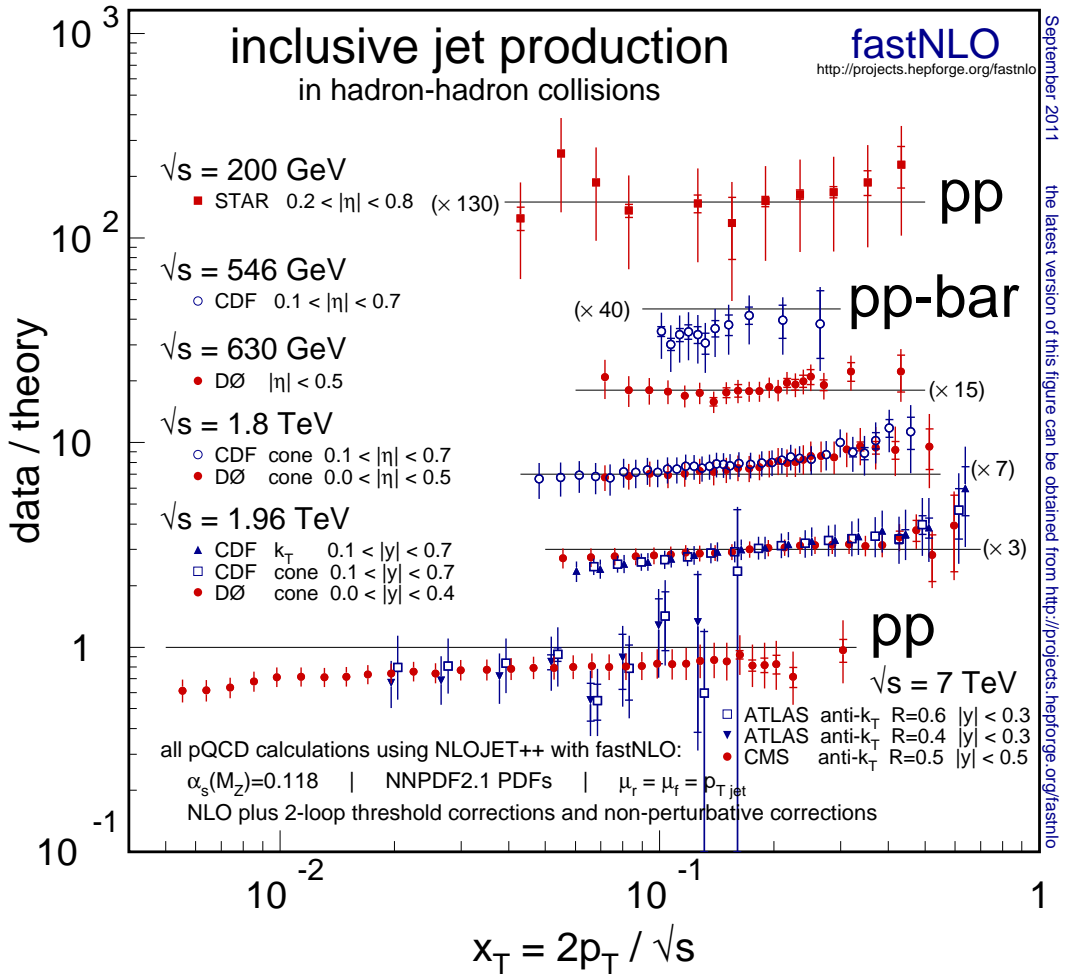


Figure 6: Ratios of data and theory for inclusive jet cross sections measured in hadron-hadron collisions at different center-of-mass energies. The ratios are shown as a function of the scaling variable $x_T = 2p_T / \sqrt{s}$. The theory results are computed for NNPDF2.1 PDFs.

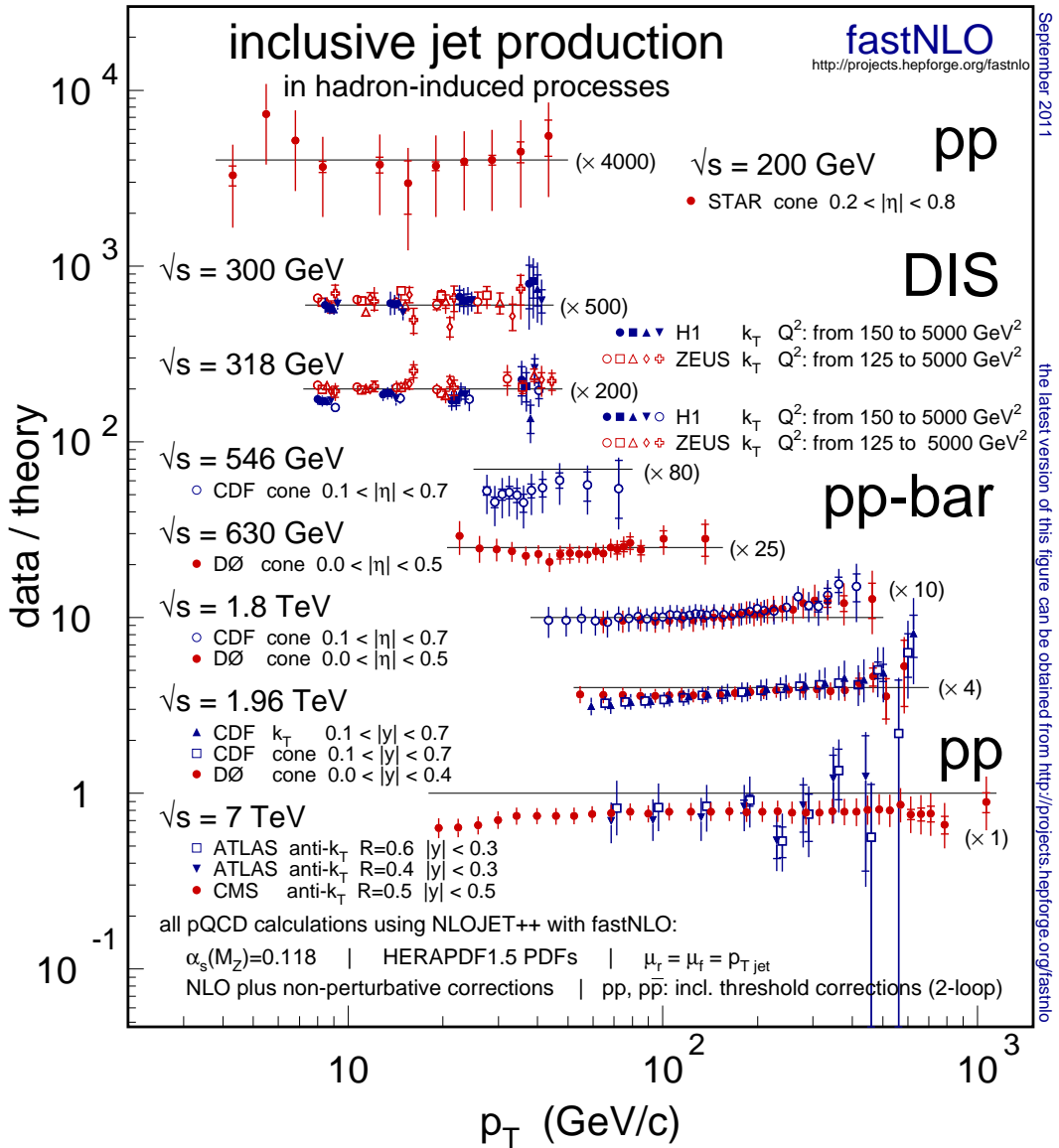


Figure 7: Ratios of data and theory for inclusive jet cross sections measured in hadron-hadron collisions and in deeply inelastic scattering at different center-of-mass energies. The ratios are shown as a function of jet transverse momentum p_T . The theory results are computed for HERAPDF1.5 PDFs.

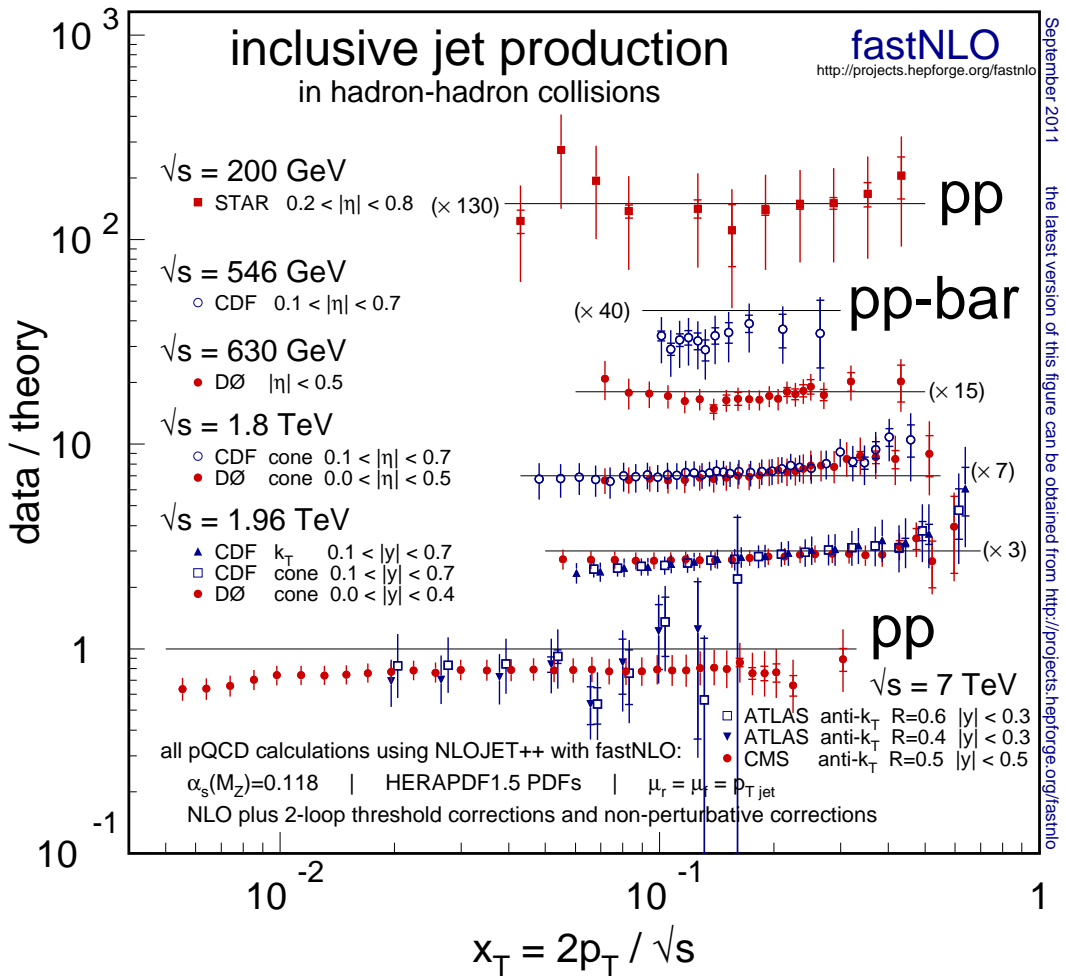


Figure 8: Ratios of data and theory for inclusive jet cross sections measured in hadron-hadron collisions at different center-of-mass energies. The ratios are shown as a function of the scaling variable $x_T = 2p_T / \sqrt{s}$. The theory results are computed for HERAPDF1.5 PDFs.